Video Article

Using Gold-standard Gait Analysis Methods to Assess Experience Effects on Lower-limb Mechanics During Moderate High-heeled Jogging and Running

Yan Zhang[1,2,3], Meizi Wang[1], Jan Awrejcewicz[3], Gusztáv Fekete[4], Feng Ren[1], Yaodong Gu[1,2]

[1]Faculty of Sports Science, Ningbo University

[2]Research Academy of Grand Health Interdisciplinary, Ningbo University

[3]Department of Automation, Biomechanics and Mechatronics, The Lodz University of Technology

[4]Savaria Institute of Technology, Eötvös Loránd University

Correspondence to: Yaodong Gu at guyaodong@hotmail.com

URL: https://www.jove.com/video/55714
DOI: doi:10.3791/55714

Keywords: Behavior, Issue 127, Moderate high heels, wearing experience, high-heeled jogging, high-heeled running, lower-limb kinematics, ground reaction force

Date Published: 9/14/2017

Citation: Zhang, Y., Wang, M., Awrejcewicz, J., Fekete, G., Ren, F., Gu, Y. Using Gold-standard Gait Analysis Methods to Assess Experience Effects on Lower-limb Mechanics During Moderate High-heeled Jogging and Running. *J. Vis. Exp.* (127), e55714, doi:10.3791/55714 (2017).

Abstract

A limited number of studies have explored lower-limb biomechanics during high-heeled jogging and running, and most studies have failed to clarify the wearing experience of subjects. This protocol describes the differences in lower-limb kinematics and ground reaction force (GRF) between experienced wearers (EW) and inexperienced wearers (IEW) during moderate high-heeled jogging and running. A three-dimensional (3D) motion analysis system with a configured force platform was used to synchronously capture lower-limb joint movements and GRF. 36 young females volunteered to participate in this study and were asked about high-heeled shoe-wearing experience, including frequency, duration, heel types, and heel heights. Eleven who had the experience of 3 to 6 cm heels for a minimum of three days per week (6 h per day) for at least two years and eleven who wore high heels less than twice per month participated. Subjects performed jogging and running at comfortable low and high speeds, respectively, with the right foot completely stepping onto a force platform when passing by along a 10 m walkway. EW and IEW adopted different biomechanical adaptations while jogging and running. IEW exhibited a generally larger range of joint movement, while EW showed a dramatically larger loading rate of GRF during running. Hence, further studies on the lower-limb biomechanics of high-heeled gait should strictly control the wearing experience of the subjects.

Video Link

The video component of this article can be found at https://www.jove.com/video/55714/

Introduction

High-heel design has always been one of the popular features of women's footwear. Forcing the ankle into a passive plantar-flexed state, high-heeled shoes considerably alter walking kinematics and kinetics. Despite reported adverse effects on the musculoskeletal system[1], social and fashion customs encourage the continued use of high-heeled shoes[2].

Optical tracking systems, currently used in the majority of gait-analysis laboratories for both clinical and research purposes, give accurate and reliable measurement of 3D lower-limb joint motions[3]. This technology provides a "gold standard" for gait analysis[4]. Consistent results based on the technique have revealed that higher heel heights lead to larger knee flexion and ankle inversion when compared with flat shoes[5,6,7]. GRF is another commonly used parameter in gait analysis. The shift of GRF toward the medial forefoot, reduced GRF during mid-stance, increased vertical GRF at heel-strike, and increased peak anterior-posterior GRF have also been observed in high-heeled walking[1,6,7,8].

Previous studies referenced above use methods based mainly on level walking. In modern society, running for a bus, darting across a busy street, or dashing to catch the last train push more and more women to use higher speeds every now and then. There are limited studies concerning lower-limb biomechanics during high-heeled jogging and running. Gu *et al.* noted that the joint motion range of knee abduction-adduction and hip flexion-extension increased significantly as the heel height increased during jogging[9]. The limitation of this study is that they only recruited habitual high-heel wearers. The frequent use of high-heeled shoes can potentially induce structural adaptions in lower-limb muscles. Zöllner *et al.* created a multiscale computational model revealing that muscle is able to gradually adjust to its new functional length due to the use of high heels after a chronic loss of sarcomeres in series[10]. Evidence also demonstrates that kinematic accommodations in gait caused by high-heeled shoes vary between experienced and inexperienced wearers[11]. Data collected from both experienced and inexperienced subjects may mask statistical results[12]. It is important to explore whether the biomechanical changes are similarly obvious in inexperienced and experienced users.

The purpose of this study was to investigate the differences in lower-limb kinematics and vertical GRF between experienced wearers (EW) and inexperienced wearers (IEW) during moderate high-heeled jogging and running. It was hypothesized that EW would show faster self-preferred jogging and running speeds, less joint motion, and larger vertical GRF during jogging and running.

Protocol

This study has been approved by the Human Ethics Committee of Ningbo University (ARGH20150356). All subjects gave their informed consent for inclusion in the study, and they were informed of the goal, requirements, and experimental procedures of the study.

1. Gait Laboratory Preparation

1. Switch off any incandescent lights and leave a reasonable fluorescent lighting level in the laboratory. Remove all markers and unwanted objects of reflection that may be misinterpreted as passive retro-reflective markers from the capture volume.
2. **Plug the appropriate dongle into the parallel port of the computer. Turn on the motion-capture cameras, proprietary tracking software, force platform amplifiers, and external analog-to-digital converter (ADC).**
    1. Allow time for the 8 cameras to initialize. Click the "Local System" node on the "System" tab of the "Resources" pane. In the "Properties" pane of the "Local System" node, type "100" into the "Requested Frame Rate" property in the "System" section to set sample rate at 100 Hz.
3. **Select "Camera" from the view list in the "View" pane. Place the T-frame, which consists of 5 markers located a fixed distance from each other, on the force platform.**
    1. In the "System Resources" tree, expand the "Cameras" node and press and hold the CTRL key while clicking each camera listed in the node. In the "Properties" pane of the "Cameras" node, move the "Strobe Intensity" bar in the "Settings" section to the left or right for each camera to ensure that data from each camera is completely, clearly, and steadily visible in the "View" pane.
4. Click the "System Preparation" button in the "Tool" pane. Click the "Start" button in the "Calibrate Cameras" section and thenphysically wave the calibration wand (T-frame) in the capture volume in a vertical figure eight whilst moving around the area intended for the capture of 3D data. Stop waving when the blue status lights on the front of the cameras stop flashing.
5. In the "Cameras Calibration Feedback" section in the "Tool" pane, monitor the progress bar until the camera calibration process is complete. Review the "Image Error" data; the acceptable image error of each camera should be less than 0.3.
6. Place the T-frame on the floor, with the central marker on the top-left corner of the force platform (60 cm × 90 cm) and the axes of the frame along the edges of the force platform. Ensure that the long axis of the frame points in the travel direction (anterior direction).
7. Select "3D Perspective" from the view list in the "View" pane. In the "Set Volume Origin" section, click the start button and click the "Set Origin" button to set the origin of the capture volume.
8. Ask a subject to step onto the force platform. Verify that the direction of the ground reaction vector displayed in the view pane is upward and that the magnitude of the vertical force component is equal to the body mass x 9.81. Ask the subject to walk away from the force platform.
9. In the "System Resources" tree, right-click on the "Force Platform" node and select "Zero Level" from the "Context" menu to calibrate the force platform. Click the "Connectivity" node on the "System" tab in the "Resources" pane. In the "Properties" pane of the "Connectivity" node, type "1,000" into the "Requested Frame Rate" property in the "Settings" section to set the sample rate at 1,000 Hz.
10. Prepare 16 passive retro-reflective markers (diameter: 14 mm) by pre-attaching them individually to one side of double-sided adhesive tape.

2. Subject Preparation

1. Organize the results of the survey about high-heel shoe-wearing experience, including frequency, duration, heel types, and heel heights, which should be given to each volunteer.
NOTE: Questions in the survey: (i) How often do you wear your high-heeled shoes? (ii) How many h/min do you wear your high-heeled shoes each time? (iii) What kind of high-heeled shoes do you usually wear? Wedge heel or stiletto heel? (iv) How high is the shoe that you usually wear? Here, 36 young females volunteered to participate in this test, but 14 of them were excluded for assorted reasons: feeling uncomfortable with the experimental shoe (4), hallux valgus (3), only having wedge-heel experience (3), abnormal gait in the experimental environment (2), and absence on the testing day (2).
2. Obtain written informed consent from subject who fulfill the inclusion criteria.
NOTE: The inclusion criteria are as follows: no musculoskeletal disorders that might affect normal jogging and running gait; feeling comfortable with the experimental shoe offered; right-foot dominant; and size 37 (EUR) EW (age: 24.2 ± 1.2 years; height: 160 ± 2.2 cm; mass: 51.6 ± 2.6 kg) wear shoes with narrow heels 3-6 cm-high for a minimum of three days per week (6 h per day) for at least two years, while IEW (age: 23.7 ± 1.3 years; height: 162.3 ± 2.3 cm; mass: 52.6 ± 4.5 kg) wear high-heeled shoes less than twice per month.
3. Ask the subjects to change into tight-fitting pants and a t-shirt.
4. Measure subjects' standing height (mm) and body mass (kg). Measure the leg length (*i.e.,* the distance between the superior iliac spine and the ankle internal condyle, in mm), knee width (*i.e.,* the distance between the medial and lateral knee condyle, in mm) and ankle width *(i.e.,* the distance between the medial and lateral ankle condyle, in mm) using measuring calipers.
5. **Prepare skin areas of anatomical bony landmarks for marker placement.**
    1. Shave body hair as appropriate and use alcohol wipes to remove excess sweat and moisturizer.
    NOTE: The marker locations include: anterior-superior iliac spine (LASI/RASI), posterior-superior iliac spine (LPSI/RPSI), lateral mid-thigh (LTHI/RTHI), lateral knee condyle (LKNE/RKNE), lateral mid-shank (LTIB/RTIB), lateral malleolus (LANK/RANK), second metatarsal head (LTOE/RTOE), and calcaneus (LHEE/RHEE), where the L and R prefixes indicate the left and ride legs, respectively.
6. Palpate to identify anatomical landmark. Circle each landmark on the skin using a marking pen. Attach the 16 passive retro-reflective markers on the landmarks of both sides of the lower limbs with double-sided adhesive tape.

7. Ask the subjects to change into the experimental shoe (heel height: 4.5 cm) and then walk, jog, and run freely along the runway until they are physiologically and psychologically comfortable with the cameras and markers on their lower limbs (*i.e.,* no influence on the participants) and they feel like they are walking, jogging, and running naturally.
8. Ask the subjects to practice jogging along the runway at a comfortable low speed until they are able to jog steadily. Instruct the subjects to perform some progressive training (*e.g.,* making an effort to jog at a progressively increasing speed on a treadmill within a safe and comfortable range).
9. Ask them to practice running on the ground along the runway at a comfortable high speed until they are able to run steadily at this speed.
10. Instruct the subjects to try to start jogging/running from different starting lines within the starting area several times to find an appropriate starting position, ensuring that the right foot naturally strikes and completely contacts the force platform when passing by.

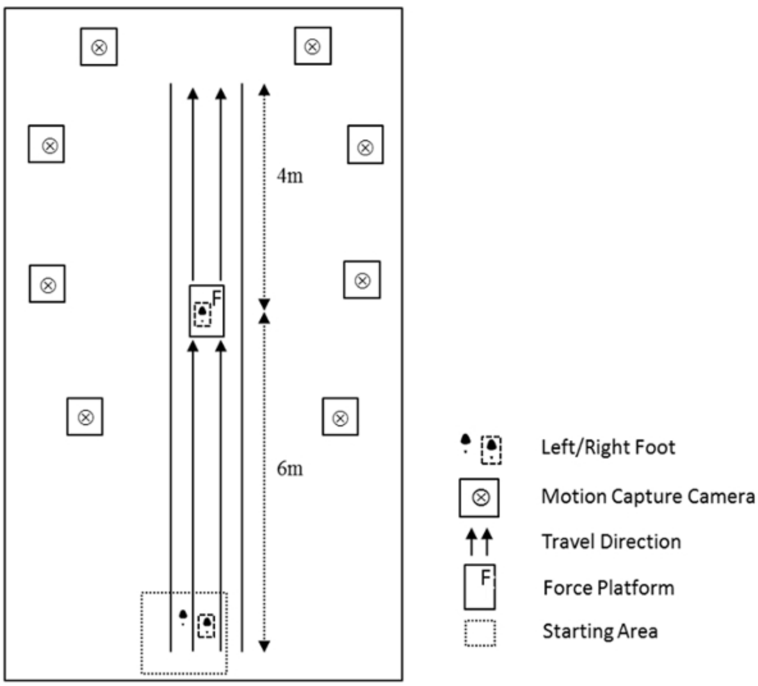

Figure 1: Experimental protocol. 8 infrared cameras capture lower-limb motion while the subject jogs and runs along the runway. The right foot naturally strikes and completely contacts the force platform when passing by. Kinematic and kinetic data were collected synchronically. Please click here to view a larger version of this figure.

3. Static Calibration

1. Click the "New Database" button in the toolbar to create a new database. Click the "Data Management" button in the toolbar to open the "Data Management" pane. In the "Data Management" pane, click the "New Patient Classification," "New Patient," and "New Session" buttons, in order. Return to the "Resources" pane, click the "Create a new subject" button to create a new subject, and enter the values for all anthropometric measurements (*e.g.,* height, weight, leg length, knee width, and ankle width) in the "Properties" pane for the newly created subject.
2. **Click the "Go Live" button in the "Resources pane." Click the "Split horizontally" button in the "View" pane and select "Graph" in the view list in the new "View" pane. Select "Trajectory Count" in the "Model Output" pulldown list.**
    1. Confirm that the count of markers in the "Graph" view pane is 16 and that the same number of markers is visible in the "3D Perspective" view pane, meaning that no markers on the lower limb have failed to be captured.
3. Click the "Subject Preparation" button in the "Tool" pane.
4. **Ask the subject to stand in a stationary neutral pose in the center of the capture volume to capture the static data.**
    1. Click the "Start" button in the subject capture section, capture approximate 150 frames, and click the "Stop" button.
    NOTE: The "Start" button switches to "Stop" automatically after clicking it.
5. Click the "Reconstruct" button in the toolbar to display the captured markers. Click the "Label" button in the "Tool" pane and manually assign the labels (16 in total) listed in the "Manual Labeling" section to the corresponding markers in the "3D Perspective" view pane. Press the "Esc" key on the keyboard to exit.
6. Select "Static" in the "Pipeline" pulldown list in the "Subject Calibration" section. Check the "Left Foot" and "Right Foot" options in the "Static Settings" pane. Click the "Start" button in the "Subject Calibration" section.

4. Dynamic Trials

1. Ask the subject to stand at the appropriate starting position.

2. Click the "Go Live" button in the "Resources" pane. Click the "Capture" button in the "Tool" pane. Edit the "Trial Name" in the "Next Trial Setup" section.
3. **Click the "Start" button in the "Capture" section to begin capturing and then immediately give the subject the oral instruction to "Go jogging/Go running." Ensure that the right foot naturally strikes and completely contacts the force platform when passing by (Figure 1).**
    1. For jogging trials, ask the subjects to jog at the comfortable low speed that they were familiar with during preparation; for running trials, ask the subjects to run at the comfortable high speed that they had been familiar with during preparation. Allow for a 2-min rest between two trials.
    2. Capture at least 3 complete successive steps, including the step on the force platform.
    NOTE: Jogging and running trials are performed randomly. For each speed, ask the subjects to repeat 5 trials. Cancel the capture in the event of a marker moving/falling or if abnormal gait occurs. In the event of markers moving/falling, re-attach to the predetermined skin mark.

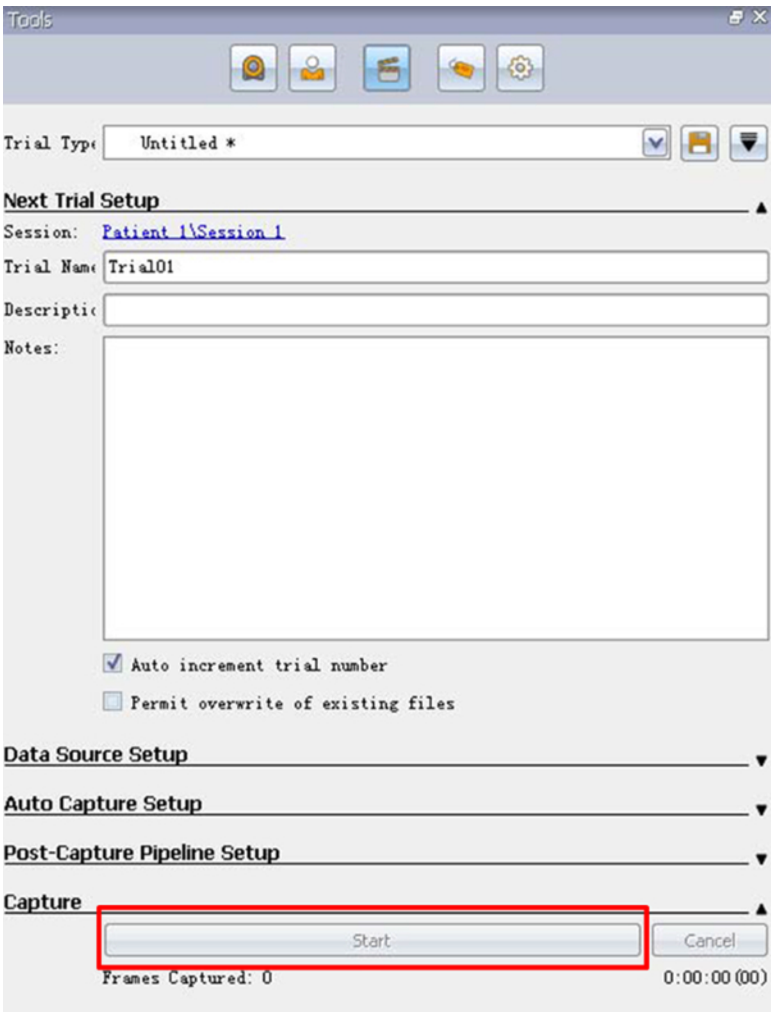

Figure 2: User interface for dynamic data collection. Please click here to view a larger version of this figure.

4. Click the "Stop" button in the "Capture" section after the subject jogs/runs to the end of the runway. See **Figure 2**.
NOTE: The "Start" button in the "Capture" section switches to "Stop" automatically after clicking it.

5. Post-processing using Proprietary Tracking Software

1. Click the "Data Management" button in the toolbar. In the "Data Management" pane, double-click the trial name. Click the "Reconstruct" and "Label" buttons in the toolbar to reconstruct the 3D dynamic model and to obtain the filmed data.
2. **On the time bar, move the left-range indicator (blue triangle) on the timeline to the frame at which the right foot strikes the force platform. Select this frame according to the instant when the vertical force vector in the view pane arises.**
    1. Move the right-range indicator (blue triangle) on the timeline to the frame at which the next heel-strike event of the right foot occurs.
    NOTE: The selection of this frame depends on the elaborative subjective estimate of the researchers according to the instant when there is no superior-inferior displacement of the right heel marker.

3. Right-click on the time bar and select "Zoom to Region-of-Interest" from the "Context" menu to define the desired frames.
4. Click the "Label" button in the "Tool" pane. In the "Gap Filling" section, click on the markers whose trajectories contain gaps listed in the "Trajectory" column and then click the "Fill" button of the "Spline Fill" tool.
NOTE: The number of gaps are listed in the "#Gaps" column. Clicking on the "Fill" button of the "Spline Fill" tool fills one gap. The "Spline Fill" method can generally be used for gap instances less than or equal to 60 frames.
5. Click the "Pipeline" button in the "Tool" pane. Select "Dynamic" from the "Current Pipeline" list. Move the indicator (blue slider) along the timeline to the last frame. Click the "Run" button to start the pipeline process and export dynamic trials in.csv format for post-processing in the data analysis software.

6. Data Analysis

1. Low-pass filter the kinematic and kinetic data using 4th-order Butterworth filters with cut-off frequencies at 10 Hz and 25 Hz, respectively[13] (see the **Table of Materials**).
2. **Divide the anterior-superior displacement of the marker on the right anterior superior iliac spine by the corresponding time to calculate the jogging/running speed.**
    1. Define the anterior-posterior displacement of the marker on right heel between the successive heel-strike events as the stride length. Define the reciprocal of the duration of the gait cycle as the stride frequency.
3. Define the difference between the peak angle and valley angle during the stance phase as the joint range of motion (ROM).
4. Calculate the vertical average loading rate by defining the slope of the vertical GRF-time curve from 20-80% of the stance time from initial contact to impact force[14].
NOTE: Define the initial contact as the instant when the vertical GRF consistently measured more than 0 N.
5. Normalize the vertical GRF to bodyweight (BW%).
6. First average the 5 trials from each subject and then average these results for all subjects.
NOTE: The parameters include jogging and running speed, stride length, stride frequency, joint (*i.e.,* ankle, knee and hip) 3D (ROM) and peak angle during stance phase, angle at heel-strike in the sagittal plane, impact force (F_i), peak force (F_p), and vertical average loading rate (VALR).
7. Transfer the data to a statistical software for statistical analysis.

7. Statistical Analysis

1. Perform two separate independent samples t-tests to assess the effects of wearing experience. Perform two separate paired-samples t-tests to assess the effects of running speed on lower-limb kinematics and GRF. Consider statistical results as significant if p <0.05.

Representative Results

All results are presented here as the mean ± standard deviation. The running speed was significantly greater than the jogging speed, regardless of wearing experience (EW: Jog *vs.* Run: 2.50 ± 0.14 *vs.* 3.05 ± 0.14, *p* = 0.010; IEW: Jog *vs.* Run: 2.24 ± 0.26 *vs.* 2.84 ± 0.29, *p* = 0.028; in m/s) (**Table 1**). No significant difference in the corresponding jogging/running speeds between EW and IEW was found. Generally, the stride length of EW was larger than that of IEW (Jog: EW *vs.* IEW: 1.86 ± 0.06 *vs.* 1.49 ± 0.20, *p* = 0.016; Run: EW *vs.* IEW: 2.15 ± 0.14 *vs.* 1.79 ± 0.16, *p* = 0.004; in m), while the stride frequency showed the opposite (Jog: EW *vs.* IEW: 82.43 ± 3.48 *vs.* 90.74 ± 2.92, *p* = 0.024; Run: EW *vs.* IEW: 85.84 ± 3.39*vs.* 96.16 ± 3.00, *p* = 0.015; in steps/min) (**Table 1**). IEW showed a significantly larger stride length (*p* = 0.025) and frequency (*p* = 0.010), and EW showed significantly larger stride length (*p* = 0.017), while running as compared to jogging.

In the sagittal plane, statistical results from paired independent t-tests showed that the ankle ROM of EW was significantly less than that of IEW (Jog: EW *vs.* IEW: 39.40±4.44 *vs.* 47.88±2.59, *p*=0.000; Run: EW *vs.* IEW: 36.16±2.42 *vs.* 43.89±3.70, *p*=0.006; in degrees) (**Figure 3**). Also, the ankle plantar-flexion at heel-strike of EW was significantly less than that of IEW (Jog: EW *vs.* IEW: -10.95 ± 2.15 *vs.* -14.34 ± 2.31, *p* = 0.014; Run: EW *vs.* IEW: -9.97 ± 0.85 *vs.* -13.63 ± 0.72, *p* = 0.011; in degrees) (**Table 3**). The knee ROM of EW during jogging was significantly larger compared to that of IEW (Jog: EW *vs.* IEW: 30.37 ± 2.11 *vs.* 29.90 ± 2.67, *p* = 0.030; Run: EW *vs.* IEW: 30.97 ± 0.86 *vs.* 30.16 ± 1.79; in degrees) (**Figure 3**). On the contrary, the knee peak flexion of EW during jogging was significantly less (Jog: EW *vs.* IEW: 39.47 ± 1.80 *vs.* 45.01 ± 2.04, *p* = 0.017; Run: EW *vs.* IEW: 42.73 ± 2.13 *vs.* 44.16 ± 2.07; in degrees) (**Table 2**). The hip peak flexion (Jog: EW *vs.* IEW: 27.70 ± 2.82 *vs.* 27.69 ± 4.00; Run: EW *vs.* IEW: 36.02 ± 2.94 *vs.* 29.15 ± 4.10, *p* = 0.000; in degrees) and flexion at heel-strike (Jog: EW *vs.* IEW: 27.54 ± 2.84 *vs.* 27.61 ± 3.92; Run: EW *vs.* IEW: 35.99 ± 2.96 *vs.* 29.09 ± 4.10, *p* = 0.000; in degrees) of EW during running were significantly larger compared to those of IEW (**Table 2** and **Table 3**). In addition, statistical results from paired sample t-tests showed that IEW presented significantly less plantar-flexion at heel-strike (Jog *vs.* Run: -14.34 ± 2.31 *vs.* -13.63 ± 0.72, *p* = 0.044; in degrees) (**Table 3**) and EW presented significantly larger hip ROM (Jog *vs.* Run: 39.22 ± 3.73 *vs.*46.12 ± 3.88, *p* = 0.010; in degrees), peak flexion (Jog *vs.* Run: 27.70 ± 2.82 *vs.* 36.02 ± 2.94, *p* = 0.000; in degrees), and flexion at heel-strike (Jog *vs.* Run: 27.54 ± 2.84 *vs.* 35.99 ± 2.96, *p* = 0.000; in degrees) while running as compared to jogging (**Figure 2**, **Table 2**, and **Table 3**).

In the frontal plane, the ankle ROM (Jog: EW *vs.* IEW: 4.90 ± 0.48 *vs.* 6.66 ± 0.26, p = 0.001; Run: EW *vs.* IEW: 5.76 ± 0.46 *vs.* 6.30 ± 0.44; in degrees) and peak inversion (Jog: EW *vs.* IEW: 5.51 ± 0.40 *vs.* 7.51 ± 0.43, p = 0.022; Run: EW *vs.* IEW: 6.80 ± 0.23 *vs.* 7.73 ± 0.33, p = 0.040; in degrees) of EW was less compared to those of IEW, and significant differences existed in the ROM during jogging and peak inversion during jogging and running (**Figure 2** and **Table 2**). The knee showed similar results to the ROM (Jog: EW *vs.* IEW: 7.23 ± 2.17 *vs.* 11.27 ± 1.20, p = 0.010; Run: EW *vs.* IEW: 9.19 ± 1.15 *vs.* 11.04 ± 1.63; in degrees) and peak abduction (Jog: EW *vs.* IEW: 4.57 ± 0.60 *vs.* 5.16 ± 0.58; Run: EW *vs.* IEW: 5.84 ± 0.69 *vs.* 7.12 ± 0.89; in degrees) with the ankle, but significant a difference only existed in the ROM during jogging (**Figure 2** and **Table 2**). As to the hip, only the peak abduction showed a significant difference between EW and IEW (Jog: EW *vs.* IEW: 6.80 ± 0.89 *vs.* 12.62 ± 1.23, p = 0.000; Run: EW *vs.* IEW: 7.73 ± 1.01 *vs.* 13.37 ± 2.07, p = 0.000; in degrees) (**Table 2**). When comparisons were made between jogging and running, the ankle peak inversion of EW (Jog *vs.* Run: 5.51 ± 0.40 *vs.* 6.80 ± 0.23, p = 0.042; in degrees) and the knee peak abduction of IEW (Jog *vs.* Run: 5.16 ± 0.58 *vs.* 7.12 ± 0.89, p = 0.017; in degrees) showed to be larger, with statistical significance during running (**Table 2**).

In the transvers plane, the running speed showed obvious effect on EW who exhibited significantly larger external rotation of the ankle (Jog *vs.* Run: -23.58 ± 1.05 *vs.* -26.82 ± 1.90, p = 0.023; in degrees) and the knee (Jog *vs.* Run: 12.13 ± 2.19 *vs.* 15.95 ± 1.62, p = 0.012; in degrees) while running as compared to jogging (**Table 2**). During running, EW also exhibited significantly less knee ROM (Jog: EW *vs.* IEW: 16.91 ± 2.21 *vs.* 18.34 ± 1.08; Run: EW *vs.* IEW: 16.26 ± 1.72 *vs.* 19.97 ± 1.26, p = 0.009; in degrees) and larger hip peak internal rotation (Jog: EW *vs.* IEW: 15.34 ± 1.53 *vs.* 14.69 ± 0.95; Run: EW *vs.* IEW: 16.91 ± 1.56 *vs.* 14.72 ± 0.99, p = 0.028; in degrees) compared to IEW (**Figure 2** and **Table 2**).

Figure 4 shows the ensemble averages of the vertical GRF under the conditions of EW-Jog, EW-Run, IEW-Jog, and IEW-Run. The GRF-time curve of EW is characterized by an initial peak immediately followed by a small wave during the shock absorption period, particularly during running. In contrast, that of IEW is relatively fluent after the initial peak. There is no significant difference in the impact force between EW and IEW, and no significant difference was observed between jogging and running (**Figure 4**). Compared with IEW, EW showed significantly larger peak force, regardless of speed (Jog: EW *vs.* IEW: 2.42 ± 0.12 *vs.* 2.05 ± 0.24, p = 0.035; Run: EW *vs.* IEW: 2.51 ± 0.14 *vs.* 2.27 ± 0.12, p = 0.042; in bodyweight). The VALR presented to be the highest under the condition of EW-Run and was significantly higher than the conditions of EW-Jog (EW-Run *vs.* EW-Jog: 102.66 ± 4.99 *vs.* 62.40 ± 10.46, p = 0.000; in bodyweight%) and IEW-Run (EW-Run *vs.* IEW-Run: 102.66 ± 4.99 *vs.* 78.15 ± 17.00, p = 0.000; in bodyweight%).

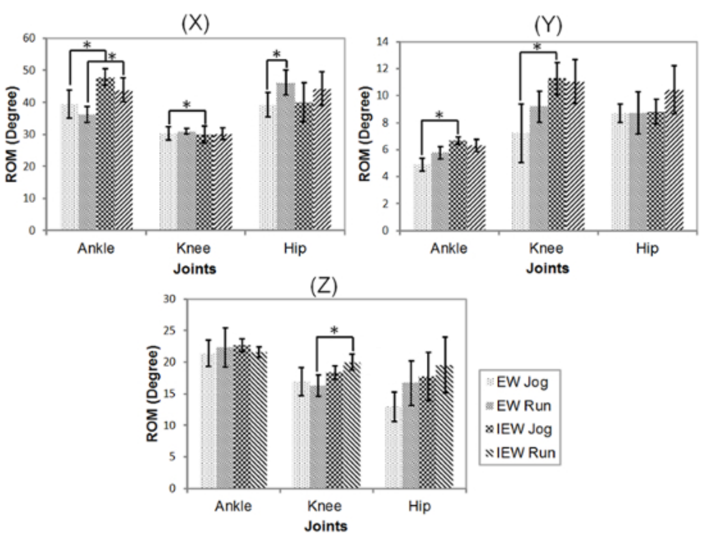

Figure 3: Joint ROM during the stance phase (EW: n=11; IEW: n=11)**.** (X) In the sagittal plane. (Y) In the frontal plane. (Z) In the transverse plane. * Statistical significance. Error bars refer to standard deviations. Please click here to view a larger version of this figure.

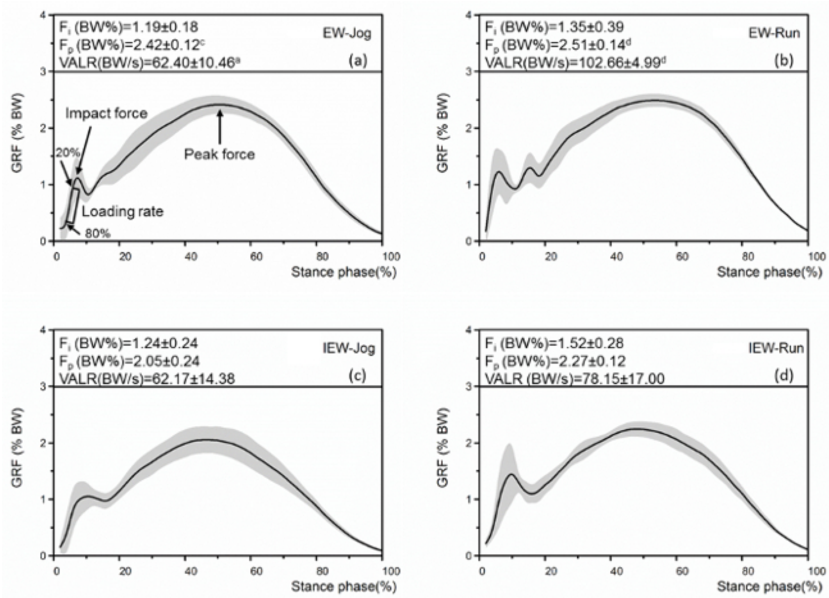

Figure 4: Ensemble averages of vertical GRF under four conditions (EW: n=11; IEW: n=11; Mean±SD)**.** (a) EW-Jog. (b) EW-Run. (c) IEW-Jog. (d) IEW-Run. The shaded areas refer to the standard deviation. F_i represents the impact force. F_p represents the peak force. VALR represents the vertical average loading rate. BW means bodyweight. [a] significant difference between EW-Jog and EW-Run; [c] significant difference between EW-Jog and IEW-Jog; [d] significant difference between EW-Run and IEW-Run. Please click here to view a larger version of this figure.

Parameters	EW (n=11)		IEW (n=11)	
	Jog	Run	Jog	Run
Speed (m/s)	2.50 ± 0.14[a]	3.05 ± 0.14	2.24 ± 0.26[b]	2.84 ± 0.29
Stride length (m)	1.86 ± 0.06[a,c]	2.15 ± 0.14[d]	1.49 ± 0.20[b]	1.79 ± 0.16
Stride frequency (steps/min)	82.43 ± 3.48[c]	85.84 ± 3.39[d]	90.74 ± 2.92[b]	96.16 ± 3.00
[a]significant difference between EW jog and EW run;	[b]significant difference between IEW jog and IEW run;	[c]significant difference between EW jog and IEW jog;	[d]significant difference between EW run and IEW run.	

Table 1: Spatio-temporal parameters (Mean ± SD).

Dimensions	Joint (Degree)	EW (n=11)		IEW (n=11)	
		Jog	Run	Jog	Run
Sagittal plane	Ankle	12.86 ± 2.10	10.64 ± 0.86	12.94 ± 1.88	10.73 ± 1.02
	Knee	39.47 ± 1.80[c]	42.73 ± 2.13	45.01 ± 2.04	44.16 ± 2.07
	Hip	27.70 ± 2.82[a]	36.02 ± 2.94[d]	27.69 ± 4.00	29.15 ± 4.10
Frontal plane	Ankle	5.51 ± 0.40[a,c]	6.80 ± 0.23[d]	7.51 ± 0.43	7.73 ± 0.33
	Knee	4.57 ± 0.60	5.84 ± 0.69	5.16 ± 0.58[b]	7.12 ± 0.89
	Hip	6.80 ± 0.89[c]	7.73 ± 1.01[d]	12.62 ± 1.23	13.37 ± 2.07
Transverse plane	Ankle	-23.58 ± 1.05[a]	-26.82 ± 1.90	-26.29 ± 1.06	-26.73 ± 0.55
	Knee	12.13 ± 2.19[a]	15.95 ± 1.62	15.44 ± 1.52	15.88 ± 0.99
	Hip	15.34 ± 1.53	16.91 ± 1.56[d]	14.69 ± 0.95	14.72 ± 0.99
[a]significant difference between EW jog and EW run;	[b]significant difference between IEW jog and IEW run;	[c]significant difference between EW jog and IEW jog;	[d]significant difference between EW run and IEW run.		

Table 2: Peak angle during the stance phase in three dimensions (Mean ± SD).

Joints (Degree)	EW (n=11)		IEW (n=11)	
	Jog	Run	Jog	Run
Ankle	-10.95 ± 2.15[c]	-9.97 ± 0.85[d]	-14.34 ± 2.31[b]	-13.63 ± 0.72
Knee	18.72 ± 5.87	24.06 ± 3.42	23.39 ± 2.22	26.34 ± 1.47
Hip	27.54 ± 2.84[a]	35.99 ± 2.96[d]	27.61 ± 3.92	29.09 ± 4.10
[a]significant difference between EW jog and EW run;	[b]significant difference between IEW jog and IEW run;	[c]significant difference between EW jog and IEW jog;	[d]significant difference between EW run and IEW run.	

Table 3: Joint angle at heel-strike in the sagittal plane (Mean±SD).

Discussion

One defect of most studies that analyze high-heeled gait biomechanics is ignoring the possible importance of experience wearing high heels[12]. This study divided subjects into groups of regular and occasional wearers to explore the effects of high-heeled shoe wearing experience on lower-limb kinematics and GRF during moderate high-heeled jogging and running.

EW and IEW showed comparable jogging/running speeds. Compared with EW, IEW adopted a higher stride frequency and a shorter stride length, which might be a strategy to maintain body balance[15,16]. The longer stride length of EW is probably associated with larger knee extension during push-off, which also increases the knee ROM in the sagittal plane. Similarly, EW exhibited a larger hip flexion-extension ROM, with increased peak flexion. This could contribute to lowering the center of mass, enhancing body stability[17]. However, the reduced ROM of the hip and knee of EW in the frontal and transverse planes could be explained as an adaptation after the long-term use of high heels to control joints from excessive motion. The more flexible ankle, with a larger ROM in the sagittal plane of IEW, serves as a less effective lever for the application of muscle force to the ground. This is a potential factor of muscle fatigue, due to the greater required muscle work to achieve a similar amount of output during the propulsive period[18].

The larger hip flexion has been reported to be a compensatory mechanism to attenuate the GRF to prevent injury[7,19]. In this study, EW exhibited larger hip peak flexion, while IEW showed larger knee peak flexion. Increased knee flexion may lead to excessive knee extensor moment[20] and rectus femoris activity[7,21], both of which are causes of knee overload[22,23]. Previous studies also reported that the higher quadricep forces induced by increased knee flexion increase proximal anterior tibial shear force, which is a major factor of anterior cruciate ligament strain[24,25]. Similarly, larger peak adduction of IEW during running may increase the medial compartment loads on the knee[26,27] and contribute to the development of knee osteoarthritis[1,23]. Coupled with the plantar-flexed position, the larger peak inversion of IEW put them at high risk of lateral ankle sprain[28]. One possible explanation for the decreased inversion of EW is the increased pronator activity caused by the long-term effect of high-heel use[15,16].

The higher impact force and loading rate during running have been considered potential factors of lower-limb injuries[29,30]. There was no significant difference in impact force observed between EW and IEW during jogging and running. However, the loading rate of EW was prominently higher during running, which was largely due to the faster transient of the force. It has been widely documented that the impact force with a rapid increasing rate would create a robust shockwave at the heel-strike event, which is then transmitted up to the lower-limb joints[31], probably causing soft-tissue injury and eventually leading to degenerative joint disorders[32]. Another key finding is that EW showed a higher peak GRF than IEW, which could contribute to increase ankle plantar flexor and pronator moments[15,16], reducing ankle instability during the propulsion period. However, the higher peak GRF also indicates higher plantar pressure on the metatarsal area. This may induce a deformity of the first metatarsophalangeal joint[33,34].

The results are dependent on a number of critical steps in the protocol. First, turning off the incandescent lights and adjusting the optimal camera strobe intensity are required to ensure the accuracy of optical 3D marker tracking. Second, camera calibration within the capture volume is important for further optimizing the motion capture accuracy. Third, locations of passive retro-reflective markers on the skin should be carefully determined and marked before attaching the markers so that the mark can be re-attached to the same location in the case of the marker moving/falling. Fourth, calibrating the force platform to the zero level before starting each dynamic trial is necessary to ensure the accuracy of the force data recording. Studies that explicate subjects' wearing experiences could provide specific information on injury reduction in targeted population. In addition to this, another advantage of this protocol presents in the data post-processing. Although the professional biomechanics analysis software is a premier tool for data management, it has its limits in terms of the graphic representation of the data. This study used an alternative to plot the data (see the **Table of Materials**). There are also limitations to this study. First, the small sample size of 11 experienced subjects and 11 inexperienced subjects may influence the statistics, resulting in non-significant differences. Second, the heel-strike event on the force platform (first frame) can be monitored in the view pane according to the instant when the force vector arises; however, the subsequent heel-strike on the ground (end frame) can only be estimated subjectively by the researchers according to the instant when there is no superior-inferior displacement of the right heel marker. The selection of this frame may vary depending on different researchers. The absence of parameters such as joint moment and joint work, which could further explain lower-limb mechanisms, is another limitation of this study.

In conclusion, regular and occasional high-heels wearers adopt different biomechanical adaptations while jogging and running. The results of this study suggest that further studies evaluating the biomechanics of high-heeled gait should carefully take into account individual wearing experience.

Disclosures

The authors have nothing to disclose.

Acknowledgements

This study is sponsored by the National Natural Science Foundation of China (81301600), K. C. Wong Magna Fund in Ningbo University, National Social Science Foundation of China (16BTY085), the Zhejiang Social Science Program "Zhi Jiang youth project" (16ZJQN021YB), Loctek Ergonomic Technology Corp, and Anta Sports Products Limited.

References

1. Barkema, D. D., Derrick, T. R., Martin, P. E. Heel height affects lower extremity frontal plane joint moments during walking. *Gait Posture.* **35** (3), 483-488 (2012).
2. Hong, W.-H., Lee, Y.-H., Chen, H.-C., Pei, Y.-C., Wu, C.-Y. Influence of heel height and shoe insert on comfort perception and biomechanical performance of young female adults during walking. *Foot Ankle Int.* **26** (12), 1042-1048 (2005).
3. Baker, R. Gait analysis methods in rehabilitation. *J Neuroeng Rehabil.* **3** (1), 1 (2006).
4. Galna, B. *et al.* Accuracy of the Microsoft Kinect sensor for measuring movement in people with Parkinson's disease. *Gait Posture.* **39** (4), 1062-1068 (2014).
5. Esenyel, M., Walsh, K., Walden, J. G., & Gitter, A. Kinetics of high-heeled gait. *J Am Podiatri Med Assocn.* **93** (1), 27-32 (2003).
6. Cronin, N. J., Barrett, R. S., Carty, C. P. Long-term use of high-heeled shoes alters the neuromechanics of human walking. *J Appl Physiol.* **112** (6), 1054-1058 (2012).
7. Mika, A., Oleksy, Ł., Mika, P., Marchewka, A., Clark, B. C. The influence of heel height on lower extremity kinematics and leg muscle activity during gait in young and middle-aged women. *Gait Posture.* **35** (4), 677-680 (2012).
8. Snow, R. E., Williams, K. R. High heeled shoes: their effect on center of mass position, posture, three-dimensional kinematics, rearfoot motion, and ground reaction forces. *Arch Phys Med Rehabil.* **75** (5), 568-576 (1994).
9. Gu, Y., Zhang, Y., Shen, W. Lower extremities kinematics variety of young women jogging with different heel height. *Int J Biomed Eng Technol.* **12** (3), 240-251 (2013).
10. Zöllner, A. M., Pok, J. M., McWalter, E. J., Gold, G. E., Kuhl, E. On high heels and short muscles: A multiscale model for sarcomere loss in the gastrocnemius muscle. *J Theor Biol.* **365** 301-310 (2015).
11. Opila-Correia, K. Kinematics of high-heeled gait with consideration for age and experience of wearers. *Arch Phys Med Rehabil.* **71** (11), 905-909 (1990).
12. Cronin, N. J. The effects of high heeled shoes on female gait: A review. *J Electromyogr Kinesiol.* **24** (2), 258-263 (2014).
13. Jones, G. D., James, D. C., Thacker, M., Green, D. A. Sit-to-stand-and-walk from 120% Knee Height: A Novel Approach to Assess Dynamic Postural Control Independent of Lead-limb. *J Vis Exp.* **114**, e54323-e54323 (2016).
14. Goss, D. L. *et al.* Lower extremity biomechanics and self-reported foot-strike patterns among runners in traditional and minimalist shoes. *J Athl Train.* **50** (6), 603-611 (2015).
15. Chien, H.-L., Lu, T.-W., Liu, M.-W. Effects of long-term wearing of high-heeled shoes on the control of the body's center of mass motion in relation to the center of pressure during walking. *Gait Posture.* **39** (4), 1045-1050 (2014).
16. Chien, H.-L., Lu, T.-W., Liu, M.-W., Hong, S.-W., Kuo, C.-C. Kinematic and Kinetic Adaptations in the Lower Extremities of Experienced Wearers during High-Heeled Gait. *BME.* **26** (3), 1450042 (2014).
17. Novacheck, T. F. The biomechanics of running. *Gait Posture.* **7** (1), 77-95 (1998).
18. Powell, D. W., Williams, D. B., Windsor, B., Butler, R. J., Zhang, S. Ankle work and dynamic joint stiffness in high-compared to low-arched athletes during a barefoot running task. *Hum Mov Sci.* **34** 147-156 (2014).
19. Robbins, S. E., Gouw, G. J., Hanna, A. M. Running-related injury prevention through innate impact-moderating behavior. *Med Sci Sports Exerc.* **21** (2), 130-139 (1989).
20. Simonsen, E. B. *et al.* Walking on high heels changes muscle activity and the dynamics of human walking significantly. *J Appl Biomech.* **28** (1), 20-28 (2012).
21. Stefanyshyn, D. J., Nigg, B. M., Fisher, V., O Flynn, B., Liu, W. The influence of high heeled shoes on kinematics, kinetics, and muscle EMG of normal female gait. *J Appl Biomech.* **16** (3), 309-319 (2000).
22. Kerrigan, D. C., Lelas, J. L., Karvosky, M. E. Women's shoes and knee osteoarthritis. *Lancet.* **357** (9262), 1097-1098 (2001).
23. Kerrigan, D. C. *et al.* Moderate-heeled shoes and knee joint torques relevant to the development and progression of knee osteoarthritis. *Arch Phys Med Rehabil.* **86** (5), 871-875 (2005).
24. Beynnon, B. D. *et al.* The strain behavior of the anterior cruciate ligament during squatting and active flexion-extension a comparison of an open and a closed kinetic chain exercise. *Am J Sports MEd.* **25** (6), 823-829 (1997).
25. Fleming, B. C. *et al.* The gastrocnemius muscle is an antagonist of the anterior cruciate ligament. *J Orthop Res.* **19** (6), 1178-1184 (2001).
26. Schipplein, O., & Andriacchi, T. Interaction between active and passive knee stabilizers during level walking. *J Orthop Res.* **9** (1), 113-119 (1991).
27. Baliunas, A. *et al.* Increased knee joint loads during walking are present in subjects with knee osteoarthritis. *Osteoarthr Cartil.* **10** (7), 573-579 (2002).
28. Payne, C., Munteanu, S., Miller, K. Position of the subtalar joint axis and resistance of the rearfoot to supination. *J Am Podiatr Med Assoc.* **93** (2), 131-135 (2014).
29. Cheung, R. T., Rainbow, M. J. Landing pattern and vertical loading rates during first attempt of barefoot running in habitual shod runners. *Hum Mov Sci.* **34** 120-127 (2014).
30. Lieberman, D. E. *et al.* Foot strike patterns and collision forces in habitually barefoot versus shod runners. *Nature.* **463** (7280), 531-535 (2010).

31. Voloshin, A., Loy, D. Biomechanical evaluation and management of the shock waves resulting from the high-heel gait: I-temporal domain study. *Gait Posture.* **2** (2), 117-122 (1994).
32. Kerrigan, D. C., Todd, M. K., Riley, P. O. Knee osteoarthritis and high-heeled shoes. *Lancet.* **351** (9113), 1399-1401 (1998).
33. Gu, Y. *et al.* Plantar pressure distribution character in young female with mild hallux valgus wearing high-heeled shoes. *J Med Mech Biol.* **14** (01), 1450008 (2014).
34. Yu, J. *et al.* Development of a finite element model of female foot for high-heeled shoe design. *Clinical Biomechanics.* **23**, S31-S38 (2008).

